

Available online at www.sciencedirect.com**ScienceDirect**

Procedia Computer Science 49 (2015) 347 – 355

Procedia
Computer Science

ICAC3'15

Modeling and Simulation of Calcium Dynamics in Fibroblast Cell involving Excess Buffer Approximation (EBA), ER Flux and SERCA Pump

Mansha Kotwani^{a *}^a*Dept of Applied Mathematics & Humanities, Thadomal Shahni Engineering College, Bandra (W), Mumbai-50*

Abstract

Computational modeling is the use of mathematics and computer science to study the behavior of complex systems by computer simulation. A computational model contains various variables that characterize the system being studied. Simulation is done by adjusting these variables and observing how the changes affect the outcomes predicted by the model. Here, a model has been developed to study complex calcium dynamics in cylindrical shaped fibroblast cell involving three important physiological parameters i.e. EBA (Excess Buffer Approximation) ER (Endoplasmic Reticulum) flux and SERCA (Sarcoplasmic Endoplasmic Reticulum ATPs) pump. The model has been developed for two dimensional unsteady state case along with appropriate initial and boundary conditions according to the physiology of the cell. Finite element technique has been employed to obtain the solution. The cytosol of the fibroblast cell is divided in to 88 elements. A computer programme has been developed in MATLAB 7.10 for the entire problem and the numerical results have been used to study the effect of buffers, ER Flux and source amplitude on calcium distribution in fibroblast cell. This model can be used to study the complex mechanisms of wound repair and tissue remodeling performed by the fibroblast cell.

© 2015 The Authors. Published by Elsevier B.V. This is an open access article under the CC BY-NC-ND license (<http://creativecommons.org/licenses/by-nc-nd/4.0/>).

Peer-review under responsibility of organizing committee of the 4th International Conference on Advances in Computing, Communication and Control (ICAC3'15)

Keywords: EBA; Buffers; ER Flux; SERCA Pump; Source Amplitude

* Corresponding author. Tel.: +919930037244.

E-mail address: manshakotwani@gmail.com

1. Introduction

Computational modeling is an emerging frontier area for research and development in the field of mathematics and computer sciences. Currently available experimental techniques for studying complex dynamic systems do not allow simultaneous studies with many system parameters. However, computational modeling of biological systems¹¹ makes possible the examination of dynamic system as a whole and the implementations of physiological functions in to artificial systems. Some of the notable examples of these physiological processes are wound healing, tissue remodeling and cell growth. The fibroblast cell plays a crucial role in these processes. These fibroblast cells secrete fibroblast growth factor (FGF), which helps the cell to proliferate^{1,2,13}. Another important factor of wound healing is the contraction of fibroblast cell³. The calcium plays an important role in triggering the functions and processes of fibroblast. In order to understand the processes of wound healing and tissue remodeling and cell growth, there is a need to understand the calcium dynamics in a fibroblast cell which involves processes like calcium diffusion, calcium buffering, influx, pump, and leak mechanisms etc. Modeling of calcium dynamics in fibroblast poses new challenges for mathematical and computational sciences and therefore it has generated interest among the researchers. The model here presented is built on mathematical and biophysical treatment of parameters obtained from experimental studies of fibroblast cell.

Some Experimental investigations are reported in the literature^{5,10,16,17} the study of calcium dynamics in fibroblast cell. Also, some attempts are reported in the literature^{6,7} for development of one and two dimensional models of calcium diffusion and regulation in presence of time dependent influx for smooth muscle cell to study the magnitude, the spatial and temporal characteristics of calcium transients in restricted diffusion spaces between the plasma membrane and intracellular organelles. But, no attempt is reported in the literature to study the effect of time dependent calcium influx on calcium dynamics in fibroblast cell involving ER flux and plasma membrane transporters with excess buffer approximation. In the view of above, here an attempt has been made to develop a two dimensional model of calcium dynamics in a cylindrical shaped fibroblast cell involving excess buffer approximation along with L-type calcium channel and endoplasmic reticulum based calcium exchange SERCA pump. Finite element method¹⁵ has been used to study the impact of various physiological parameters on calcium dynamics in fibroblast cell. MATLAB program has been developed for graphical representation of these finite element results in two dimensional plots.

2. Mathematical Model

The model cell geometry of fibroblast cell is of cylindrical shape with a maximal diameter^{16,17} of 10 μm . The shape was simplified in to cylinder that had a same diameter. The model allows the diffusion along radial and angular direction only. Thus the calcium diffusion in fibroblast cell involving excess buffer approximation with ER flux and SERCA pump (see Fig. 1.) can be rewritten for a two dimensional unsteady state case in polar cylindrical co-ordinates⁴ as given below:

$$\frac{\partial [Ca^{2+}]}{\partial t} = D_{Ca} \left(\frac{1}{r} \frac{\partial}{\partial r} \left(r \frac{\partial [Ca^{2+}]}{\partial r} \right) + \frac{1}{r} \frac{\partial}{\partial \theta} \left(\frac{1}{r} \frac{\partial [Ca^{2+}]}{\partial \theta} \right) \right) - k_j [B]_{\infty} ([Ca^{2+}] + [Ca^{2+}]_{\infty}) + \frac{A_{ER}}{V_{ER}} K_{IP3R} ([Ca_{ER}^{2+}] - [Ca^{2+}]) + \frac{A_{ER}}{V_{ER}} ([Ca_{ER}^{2+}] - [Ca^{2+}]) - \frac{A_{ER}}{V_{ER}} \frac{J_{SERCA}^{\max}}{K_{SERCA}} [Ca^{2+}] \quad (1)$$

All the parameters and their values are given in table [1]. It is assumed that the centre of circle is at ($r = 0, \theta = 0$) and radius of circle is $r = 5 \mu\text{m}$, see Fig 1. The point source is situated at ($r = -5, \theta = \pi$) and as we move away from the source the calcium concentration in cytosol achieves its background value i.e. $0.1 \mu\text{M}$. So the boundary condition takes the following form^{8,12,20}:

$$\lim_{\substack{r \rightarrow -5 \\ \theta \rightarrow \pi}} \left(-2\pi r D_{Ca} \frac{\partial [Ca^{2+}]}{\partial r} \right) = \sigma_{Ca} \quad (2)$$

Where σ_{Ca} denotes the time dependent opening and closing of surface membrane Ca channels and it is represented by the following expression^{6,7}

$$\sigma_{Ca} = P_0 (1 - \exp(-t/T_{on})) (\exp(-t/T_{off})) \quad (3)$$

Where P_0 is the permeability constant and T_{on}, T_{off} are time constant. All the parameters were adjusted so that the maximum concentration during the transient matched the current records in the literature¹⁹.

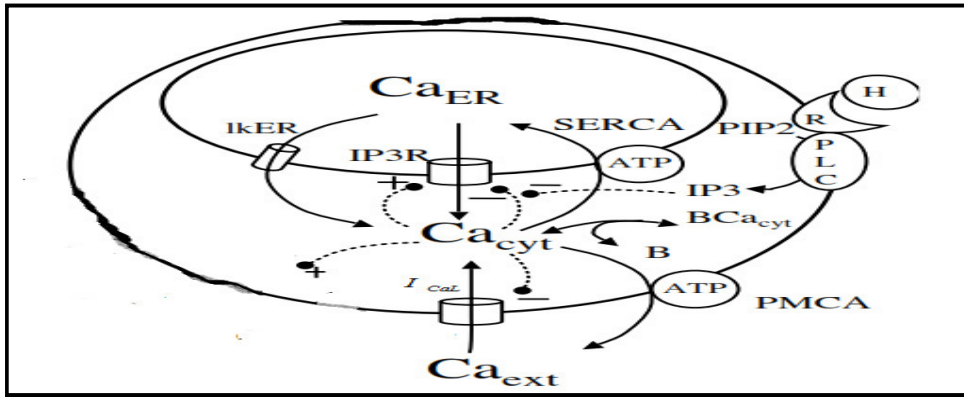


Fig. 1. An overview of complete intracellular calcium dynamics model in fibroblast cell⁹

For other boundary condition, it is assumed that $[Ca^{2+}]$ attains its steady state concentration $0.1\mu M$ as we move far away from the source;

$$\lim_{r \rightarrow 5, \theta \rightarrow 2\pi} [Ca^{2+}] = [Ca]_{\infty} \quad (4)$$

For our convenience we are writing 'u' in lieu of $[Ca^{2+}]$. Here we are using the finite element method¹⁵, for space discretization (See Fig. 2.) and backward difference method for time derivative.

The discretized variational form¹⁵ of equations (1) to equation (4)

$$I^{(e)} = \frac{1}{2} \iint_A \left\{ r \left(\frac{du^{(e)}}{dr} \right)^2 + \frac{1}{r} \left(\frac{du^{(e)}}{d\theta} \right)^2 + \frac{1}{D_{Ca}} (\eta u^{(e)2} - 2\gamma u^{(e)}) r + \frac{1}{D_{Ca}} r u^{(e)} \frac{\partial u^{(e)}}{\partial t} \right\} dA - \mu^{(e)} \left(\frac{\sigma_{Ca}}{2\pi D_{Ca}} u^{(e)} \Big|_{r=5} \right) \quad (5)$$

Where 'e' denotes the number of elements i.e. $e=1, 2, \dots, 80$. Also the second term ($\mu(e)=1$) for $e=40, 50$ and ($\mu(e)=0$) for rest of the elements. Here

$$\eta = k_j^+ [B]_\infty + \frac{A_{ER}}{V_{ER}} K_{IP_3R} + \frac{A_{ER}}{V_{ER}} K_{lKER} + \frac{A_{ER}}{V_{ER}} \frac{J_{SERCA}^{\max}}{K_{SERCA}}$$

$$\text{and } \gamma = k_j^+ [B]_\infty u_\infty + \frac{A_{ER}}{V_{ER}} K_{IP_3R} u_{ER} + \frac{A_{ER}}{V_{ER}} K_{lKER} u_{ER}$$

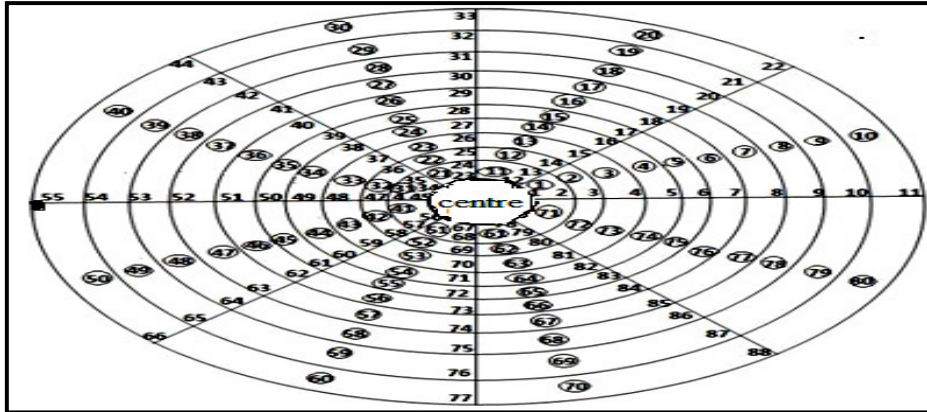


Fig. 2. Finite element discretization of cytosol, here the numbers in circle represents the elements and without circle represents the nodal points and the small dark circle on the left side (at the nodal point 55) represent the point source

The following bilinear shape function for the calcium concentration within each element has been taken as¹⁵ :

$$u^{(e)} = c_1^{(e)} + c_2^{(e)} r + c_3^{(e)} \theta + c_4^{(e)} r\theta \quad (6)$$

$$u^{(e)} = P^T c^{(e)} \quad (7)$$

where, $P^T = [1 \quad r \quad \theta \quad r\theta]$ and $(c^{(e)})^T = [c_1^{(e)} \quad c_2^{(e)} \quad c_3^{(e)} \quad c_4^{(e)}]$ From equation (6) & (7) we get,

$$\overline{u^{(e)}} = P^{(e)} c^{(e)} \quad (8)$$

$$\text{Where, } \overline{u^{(e)}} = \begin{bmatrix} u_i \\ u_j \\ u_k \\ u_l \end{bmatrix} \quad \text{and} \quad P^{(e)} = \begin{bmatrix} 1 & r_i & \theta_i & r_i \theta_i \\ 1 & r_j & \theta_j & r_j \theta_j \\ 1 & r_k & \theta_k & r_k \theta_k \\ 1 & r_l & \theta_l & r_l \theta_l \end{bmatrix}$$

From equation (8) we have,

$$c^{(e)} = R^{(e)} \overline{u^{(e)}} \quad (9)$$

where, $R^{(e)} = P^{(e)-1}$

Substituting $c^{(e)}$ from equation (9) in equation (7) we get,

$$u^{(e)} = P^T R^{(e)} \overline{u^{(e)}} \quad (10)$$

Now, the integral $I^{(e)}$ can be in the form

$$I^{(e)} = I_k^{(e)} + I_m^{(e)} + I_\lambda - I_s^{(e)} - I_z^{(e)} \quad (11)$$

Where,

$$I_k^{(e)} = \frac{1}{2} \int_{\theta_i}^{\theta_k} \int_{r_i}^{r_j} \left[r \left(\frac{du^{(e)}}{dr} \right)^2 + \frac{1}{r} \left(\frac{du^{(e)}}{d\theta} \right)^2 \right] dr d\theta$$

$$I_m^{(e)} = \frac{1}{2} \int_{\theta_i}^{\theta_k} \int_{r_i}^{r_j} \left[\frac{1}{D_{Ca}} \eta u^{(e)2} r \right] dr d\theta$$

$$I_s^{(e)} = \int_{\theta_i}^{\theta_k} \int_{r_i}^{r_j} \left[\frac{1}{D_{Ca}} \gamma u^{(e)} r \right] dr d\theta$$

$$I_\lambda^{(e)} = \frac{1}{2} \int_{\theta_i}^{\theta_k} \int_{r_i}^{r_j} \left[\frac{1}{D_{Ca}} r u^{(e)} \frac{\partial u^{(e)}}{\partial t} \right] dr d\theta$$

$$I_z^{(e)} = \mu^{(e)} \int_{\theta_i}^{\theta_j} \left(\frac{\sigma}{2\pi D_{Ca}} u^{(e)} \right)_{r=5} d\theta$$

Thus, we can write,

$$\frac{dI^{(e)}}{du^{(e)}} = \frac{dI_k^{(e)}}{du^{(e)}} + \frac{dI_m^{(e)}}{du^{(e)}} + \frac{dI_\lambda^{(e)}}{du^{(e)}} - \frac{dI_s^{(e)}}{du^{(e)}} - \frac{dI_z^{(e)}}{du^{(e)}} \quad (12)$$

Using equation (12), we get,

$$\frac{dI}{du} = \sum_{e=1}^N \overline{M}^{(e)} \frac{dI^{(e)}}{du^{(e)}} \overline{M}^{(e)T} \quad (13)$$

$$\text{Where, } \overline{M}^{(e)} = \begin{bmatrix} 0 & 0 & 0 & 0 \\ \cdot & \cdot & \cdot & \cdot \\ 1 & 0 & 0 & 0 \\ 0 & 1 & 0 & 0 \\ 0 & 0 & 1 & 0 \\ 0 & 0 & 0 & 1 \\ \cdot & \cdot & \cdot & \cdot \\ 0 & 0 & 0 & 0 \end{bmatrix} \text{ and } I = \sum_{e=1}^{80} I^{(e)} \quad (14)$$

The integral I is extremized with respect to each nodal calcium concentration u_i ($i=1, 2, \dots, 88$). After, rearranging the equations and writing in matrix form, we have a system of ordinary differential equation

$$[K]_{88 \times 88} [\bar{u}]_{88 \times 1} + [M]_{88 \times 1} \left[\frac{d\bar{u}}{dt} \right]_{88 \times 1} = [F]_{88 \times 1} \quad (15)$$

Here, $\bar{u} = u_1 u_2 \dots \dots \dots u_{88}$, $[K]$ and $[M]$ are the system matrices and $[F]$ is the system vector. The system (15) is solved using backward difference method. The time taken for simulation is nearly 2 min on aforesaid computer. The numerical results are computed using a programme developed in MATLAB using 7.10 on a intel (R) Core (TM) 2Duo CPU, 4.00 GB RAM, 2.00 GHz processor.

3. Results & Discussion

This section shows the results from model simulation of distribution of calcium concentration in two dimensions. To simulate the model of calcium dynamics in fibroblast cell involving the important physiological parameters a MATLAB programme has been developed. The numerical values of physical and physiological parameters used for the computation of numerical results are given in table [1].

Table 1. Values of physiological parameter

Symbol	Parameters	Values	Reference
$[B_{\infty}]$	Buffer concentration	$20 \mu M$	[9]
$[Ca^{2+}]_{\infty}$	Background calcium concentration	$0.1 \mu M$	Physiological facts
J_{SERCA}^{\max}	Maximal pump rate of SERCA	$1.6 \times 10^{-5} \frac{\mu mol}{(s \times dm^2)}$	[9]
K_{SERCA}	SERCA calcium dissociation constant	$0.20 \mu M$	[9]
K_{lER}	Leak constant	$2.0 s^{-1}$	[9]
$[Ca^{2+}]_{ER}$	Endoplasmic reticulum calcium concentration	$10.89 \mu M$	[9]
A_{PM}	Plasma membrane area	$2 \times 10^{-7} dm^2$	[9]
A_{ER}	Endoplasmic reticulum area	$0.3 \times 10^{-7} dm^2$	[9]
V_{ER}	Volume of ER	$0.1 \times 10^{-12} dm^3$	[9]
D_{Ca}	Diffusion Coefficient	$250 \mu m^2 / second$	[18]
k_j^+ (EGTA)	Buffer association rate (Exogenous buffer)	$1.5 \mu M^{-1} second^{-1}$	[8,20]

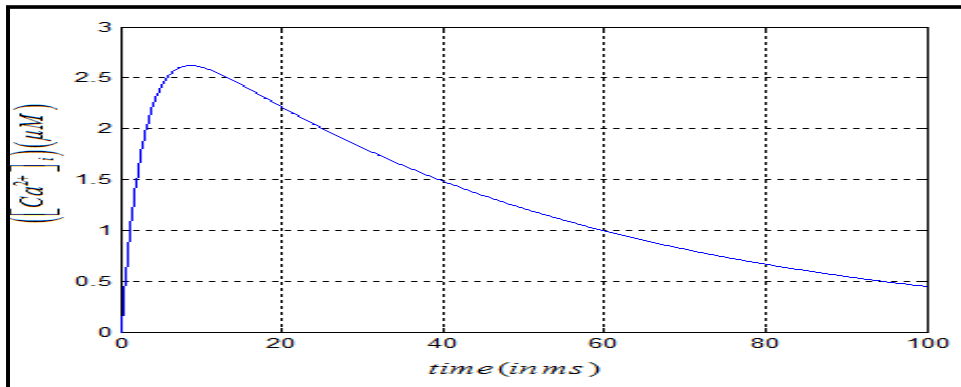


Fig. 3. Calcium concentration profile in fibroblast cell along time at $r = 5 \mu m, \theta = \pi$

Fig.3 shows the cytosolic calcium concentration with respect to time near open calcium channel. It is observed that initially the cytosolic calcium concentration increases rapidly with time and after that it decreases exponentially till $t=100$ ms. The maximum calcium concentration is $2.6 \mu M$ at $t=10$ ms in the presence of open calcium channel and closure of calcium channel results the rapid decrease in calcium concentration. The maximum slope is observed in the above fig. between $t=20$ ms to $t=40$ ms. The reason behind the sudden fall in cytosolic calcium concentration is the fast activities of calcium buffer near the open channel. After $t=40$ ms the calcium concentration decreases gradually and achieves background calcium concentration value after $t=100$ ms. Therefore, time dependent calcium influx plays very important role to perform wound healing functions properly in fibroblast cell .

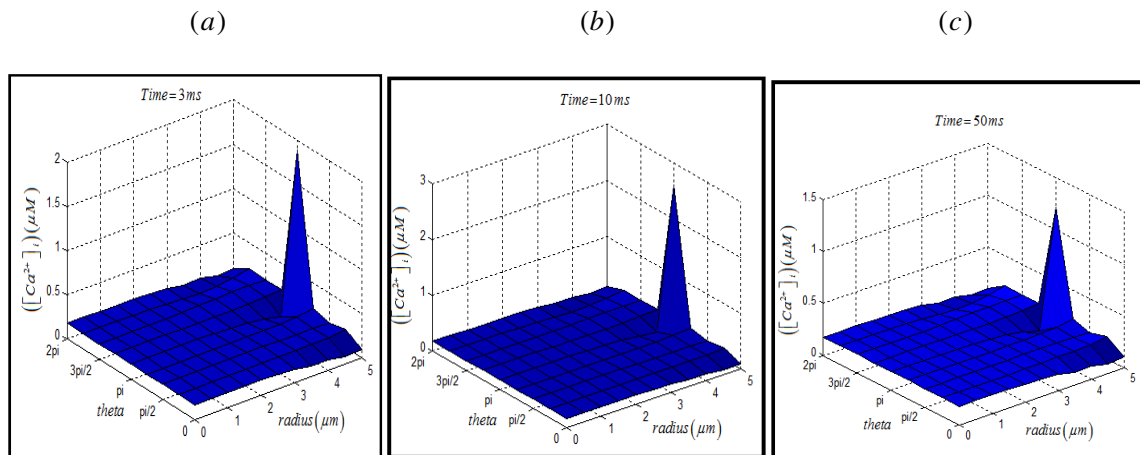


Fig. 4. Spatial calcium concentration profile for time (a) $t=3$ ms, (b) $t=10$ ms (c) $t=50$ ms

Fig. 4 shows the spatial calcium concentration profile for time $t=5$ ms, $t=10$ ms and $t=50$ ms in the presence of ER flux, L-type calcium channel, and SERCA pump with excess buffer approximation. It is observed from the above

figure that maximum calcium concentration is at $r = 5 \mu m, \theta = \pi$ i.e. near the open channel. The calcium concentration falls sharply after $r = 5 \mu m$ and achieves background concentration of $0.1 \mu M$. The peak calcium concentration in fig 4(b) is higher than that in fig. 4(a) and 4(c). This is because the activation of time dependent calcium influx at $t = 10$ ms in the above model. While Kargacin et al⁷ demonstrated that the calcium concentration near the membrane reaches $2 \mu M$ in 20 ms upon the activation of time dependent calcium influx through plasma membrane channel present in smooth muscle cell. It takes longer time period to reach maximum cytosolic calcium concentration in their model because it allows the diffusion in restricted space and our model predicts the free diffusion of calcium in two dimensions not restricted between the plasma membrane and the intracellular organelles.

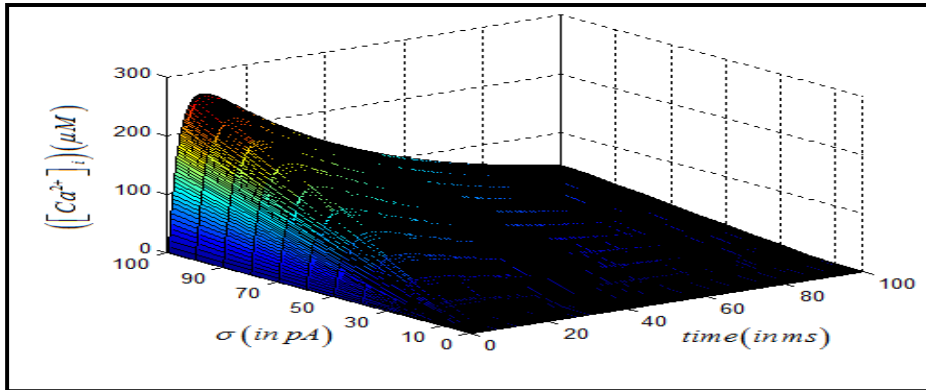


Fig.5. Calcium concentration profile with respect to source amplitude near open calcium channel ($r = 5 \mu m, \theta = \pi$) and time

Fig. 5 shows the calcium concentration profile near the open Calcium channel. It is observed from the above figure that in the absence of time dependent calcium influx the calcium concentration is at the background calcium concentration i.e. $0.1 \mu M$. Also in the presence of calcium influx as source amplitude increases the calcium concentration in cytosol increases proportionally. This shows that intensity of source amplitude is as important as in the case of constant calcium influx from the plasma membrane channel.

(a)

(b)

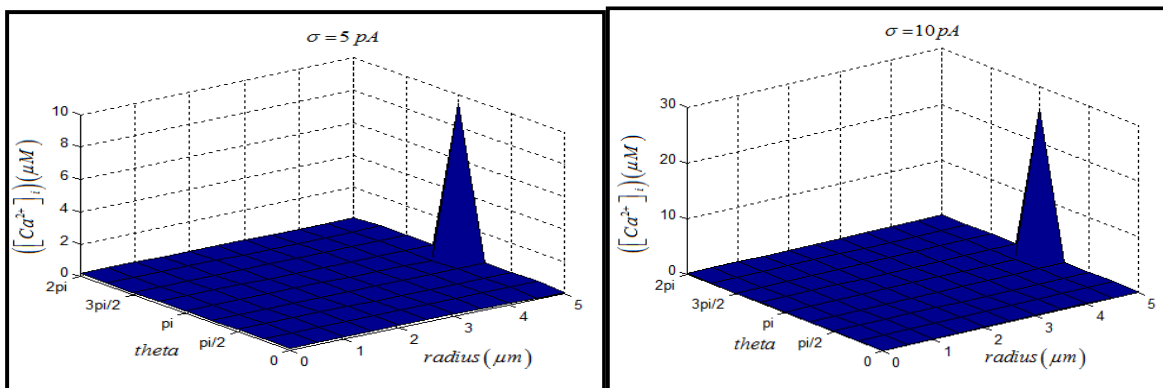


Fig. 6. Spatial calcium concentration profile at $t = 10$ ms for (a) $\sigma = 5$ pA, (b) $\sigma = 10$ pA.

Fig.6 shows the calcium concentration distribution in two dimensions at $t = 10$ ms. It is observed from the Figure that the calcium concentration rises sharply at $(r = 5 \mu\text{m}, \theta = \pi)$, when the calcium channel is open near the plasma membrane. It can be concluded from the fig 6 that the maximum calcium concentration in Fig. 6 (b) is almost twice as that of Fig. 6 (a). This implies that the rise in calcium concentration are in the ratio of source amplitude. To evoke an action potential in single NRK fibroblast cell, much higher current pulse is necessary than that in cluster of cells⁵. The present model depicts that 2 pA current is sufficient to evoke action potential in single NRK cell. While this value is quite lower as compared to constant calcium influx of point source and line source^{8,14}. Thus, it concluded that the calcium concentration increases proportionally for increasing values of source amplitude irrespective of time dependent calcium influx or time dependent calcium influx.

4. CONCLUSION

Coaxial circular sector based finite element approach was developed and employed to study calcium diffusion for two dimensional cases in a fibroblast cell in this model. This approach gives us comparably good approximation of the complex geometry of the cell including various biophysical parameters like ER flux, receptors, Pumps, leak and Plasma membrane calcium channels. These models were employed to study various physiological processes in cell. The study of time dependent calcium influx on calcium dynamics performed by using the finite element method gives us new insight of the calcium patterns in a fibroblast cell. Such models can be further developed to get better insight of Spatio-temporal calcium concentration patterns in fibroblast cell under various normal and abnormal conditions. The information generated from these models may of great use to biomedical scientists for understanding the structure and processes of fibroblast cells in wound healing, tissue remodeling and growth.

References

1. Balk SD, Whitfield JF, Youdale T and Braun AC. Roles of calcium serum, plasma and folic acid in the control of proliferation of normal and rous sarcoma virus infected chicken fibroblasts. *Paroc. Natl Acad Sci (USA)* 1973;**70**: 675-679.
2. Balk SD, Polimeni P I, Hoon BS, Le Sturgeon DN and Mitchell RS. Proliferation of Rous Sarcoma virus infected, but not of normal, chicken fibroblasts in a medium of reduced calcium and magnesium concentration. *Proc Natl Acad Sci (USA)* 1979;**76**: 3913-3916.
3. Clark RAF. Wound repair-Curr.Opin. *Cell Biol* 1989;**1**:1000-1008.
4. Crank J. *The Mathematics of Diffusion*. 2nd ed. Oxford Press; 1975.
5. Harks EG, Torres JJ, Cornelisse LN, Ypey DL and Theuvenet AP. Ionic basis for excitability of normal rat kidney (NRK) fibroblasts. *J Cell Physiology* 2003c;**196**:493-503.
6. Kargacin GJ, Fay S. Fredric, Calcium Movement in Smooth Muscle Cells Studied with One and Two-dimensional Diffusion Models. *Biophysical Journal* 1991;**60**:1088-1100.
7. Kargacin GJ. Calcium Signaling in Restricted Diffusion Spaces. *Biophysical Journal* 1994;**67**: 262-272.
8. Kotwani M, Adlakha N, Mehta MN. Finite Element Model to Study the Effect of Buffers, Source Amplitude and Source Geometry on Spatio-temporal Calcium Distribution in Fibroblast cell. *Journal of Medical Imaging and Health Informatics* 2014;**4**(6): 840-870.
9. Kusters JMAM, Dermonson MM, Van Meerwijk WPM, Ypey DL, Theuvenet APR, and Gielen CCAM. Stabilizing Role of Calcium Store-dependent Plasma Membrane Calcium Channels in Action Potential Firing and Intracellular Calcium Oscillations. *Bio Phys. J* 2005;**89**: 3741-3756.
10. Kusters JMAM, Cortes JM, Van Meerwijk WPM, Ypey DL, Theuvenet APR, and Gielen CCAM. Hysteresis and Bi-Stability in a Realistic Cell-model for Calcium Oscillations and Action Potential Firing. *Phys Rev Lett* 2007;**98**:98-107.
11. Murray JD. *Mathematical Biology*. 3rd ed. Springer; 2001.
12. Neher E. Concentration profiles of intracellular Ca^{2+} in the presence of diffusible chelator. *Exp Brain Res Ser* 1986;**14**: 80-96.
13. Nobe K, Nobe H, Obara K, Paul RJ. Preferential role of intercellular Ca^{2+} Stores in regulation of isometric force in NIH3T3 fibroblast fibres. *journal of physiology* 2000; **529**:669 – 679.
14. Pandey Sunil, Pardasani KR . Finite element model to study effect of advection diffusion and $\text{Na}^+/\text{Ca}^{2+}$ exchanger on Ca^{2+} distribution in Oocytes. *Journal of Medical Imaging and Health Informatics* 2013; **3**(3): 374-379.
15. Rao SS. *The Finite Element Method in engineering*, Elsevier Science and Technology books;2004.
16. Ross De ADG, Willems PH, Zoelen Van EJ and Theuvenet AP. Synchronized Ca^{2+} signaling Mediated by intercellular propagation of Ca^{2+} action potential in monolayer of NRK Fibroblasts. *Am J Physiol* 1997d;**273**: C1900-1907.
17. Ross De ADG, Willems PH, Zoelen Van EJ and Theuvenet AP. Synchronized calcium spiking resulting from spontaneous calcium action potentials in monolayers of NRK fibroblasts. *Cell Calcium* 1997c;**22**:195-207.
18. Tiwari S, and Pardasani KR. Finite difference model to study the effects of Na^+ influx on cytosolic Ca^{2+} diffusion. *International journal of Biological and Medical Sciences* 2009;**1**:205-209.
19. Torres JJ, Cornelisse LN, Harks EGA, Ypey DL, and Theuvenet AP. Modelling Action Potential Generation and Propagation in NRK Fibroblasts. *AM J Physiol, Cell Physiol* 2004;**287**:851-865.
20. Tripathi A and Adlakha N. Finite Volume Model to Study Calcium Diffusion In Neuron Cell Under Excess Buffer Approximation. *International J. of Math. Sci. & Engg. Appls. (IJMSEA)* 2011;**5**(3): 437-447